JCTC Journal of Chemical Theory and Computation

Chiral Aromaticities. A Topological Exploration of Möbius Homoaromaticity

Charlotte S. M. Allan and Henry S. Rzepa*

Department of Chemistry, Imperial College London, South Kensington Campus, London SW7 2AZ, U.K.

Received May 27, 2008

Ⓦ **This paper contains enhanced objects available on the Internet at http://pubs.acs.org/JCTC.**

Abstract: A series of C_2-symmetric homoderivatives of the cyclo $C_9H_9^+$ cation first identified by Schleyer as Möbius aromatic are shown to themselves sustain Möbius 4n-π-electron homoaromaticity. Analogous double-twist Möbius bis-homoaromatics follow a 4n+2 electron rule. AIM (atoms-in-molecules) and ELF (electron localization function) analysis of the electron topology in the region of the homobond of these systems reveals that the presence of a AIM bond-critical point in this region is not mandatory, it being unstable to subtle variations in the local electron density induced by local or remote substituents, and which can in turn induce self-annihilation or creation of a pair of bond and ring critical points. The same substituent-induced annihilation/creation of such a BCP/RCP pair can also be observed in the nonclassical norbornyl cation. We suggest that the ELF and ELF_π thresholds for any basin found in the homoregion are better indicators of the delocalized nature of the homoaromatic interaction and the aromaticity of the system.

1. Introduction

Homoaromaticity is a term introduced by Winstein[1] in 1959 to describe systems in which the σ framework of a cyclic conjugated and planar aromatic (4n+2) π-electron framework is interrupted with one or more bridging groups (predominantly but not necessarily manifested by CH_2). This results in through space rather than through bond overlap of the p_π-p_π framework. Since then a large body of work has concluded that the phenomenon manifests best in cationic systems, of which the homotropylium ion **1** is held as the archetypal example.[2] Homoaromaticity as described by Winstein has thus far been exclusively interpreted in terms of achiral benzenoid models in which the p_π-p_π overlaps occur with preservation of an (idealized) plane of symmetry, the so-called Hückel aromaticity model. Yet there is another model, a chiral (dissymmetric) one characterized as having (idealized) axes of symmetry only, and which has become known as the 4n-electron Möbius aromaticity model.[3] This distinction was first clearly introduced as a convenient selection rule for the transition states of organic pericyclic reactions[4] in 1966. Only in the past decade however has it has been extended to characterized examples of stable organic Möbius-aromatic molecules.[5] Most recently further diversification to a variety of organometallic, metallacyclic, and inorganic substances has been reported.[6] The first (and still one of the best) examples of cyclic Möbius π-conjugation to be identified is the $C_9H_9^+$ cation, shown by Schleyer[7] to be an 4n eight π-electron delocalized and chiral aromatic cycle **2** bearing a C_2 axis of symmetry only. Here we extend the diversity of Möbius behavior to that of Möbius homoaromaticity, using as the starting point a theoretical exploration of systems derived from **2**.

2. Results and Discussion

2.1. The Möbius Homoaromatic 3, X=CH$_2$. Combining the characteristics of **1** and **2** results in the C_2-symmetric 8-π-electron **3** (X=CH_2), in which the π system undergoes a half-twist in the cycle. Any homoaromaticity would be defined by the degree of conjugation sustained across the C1−C9 bond in this species and whether any resulting ring current in the system is strongly diatropic. The latter is most simply quantified by the NICS index introduced by Schley-

* Corresponding author e-mail: rzepa@ic.ac.uk.

10.1021/ct8001915 CCC: $40.75
Published on Web 10/15/2008

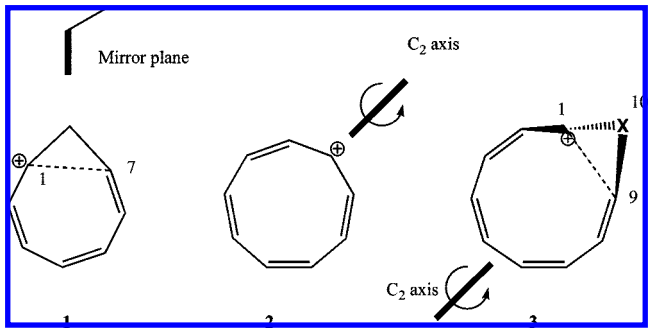

er.[8] Preliminary results for the prototypic system **3**, X=CH_2 were reported elsewhere,[9] B3LYP/6−31G(d,p) calculations indicating that the C1−C9 bond was surprisingly short (Web-enhanced Table 1), but that this value was *also* associated with a low degree of bond length alternation (i.e., geometric delocalization) in the ring defined by the sp^2-hybrid carbon atoms. This alternation can be simply approximated by specifying the difference between the shortest and longest bonds in this cycle (Δ_r) and has the value of 0.035 Å in this instance. If in fact the structure was better represented by the bicyclic isomer **4** (with a formal σ-single bond between C1−C9), the interrupted delocalization would only extend between C2−C8, and the C1−C2 bond would also be close to a single bond in length (it actually has a predicted value of 1.419 Å, close to the typical aromatic value in benzene). This aspect can be tested further by calculating the anion of **3**, X=CH_2, which as a 4n+2 10-electron half-twist system would yield a Möbius homoantiaromatic. The molecule avoids this (high energy) solution by instead adopting the anionic form of **4**, for which the C1−C9 and C1−C2 bonds are indeed both long (1.502 and 1.480 Å, respectively, Δ_r 0.113Å) and sustaining eight acyclic rather than ten cyclically conjugated π-electrons. Winstein has previously noted analogous behavior for metallocomplexes of **1**.[10] Thus while **1** as coordinated by $Cr(CO)_3$ (a 6π-acceptor) is genuinely homoaromatic, when the ligand is replaced by $Fe(CO)_3$ (a 4π-acceptor), the complex instead adopts the bicyclic form with a formal single bond between C1−C7.

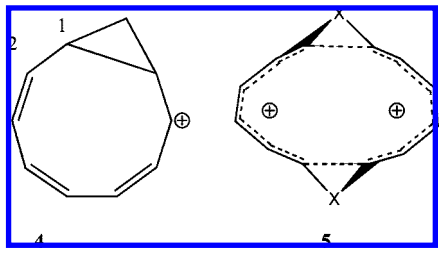

To characterize the nature of the C1−C9 bond in **3** (X=CH_2), we used Bader's critical point analysis[11] of the electron density (AIM) and the related ELF[12] (electron localization function). AIM (Atoms-in-molecules) involves analysis of the rate of curvature (Laplacian) of the electron density ρ(r) in terms of four types of so-called critical points, at each of which the derivative of ρ(r) is zero. These four are nuclear critical points (located at the nuclei), bond critical points (BCP) located between (normally pairs of) nuclei, ring critical points (RCP, defining a ring of nuclei), and cage critical points (CCPs). A topological relationship (the Poincaré-Hopf rule) between the numbers of each type of critical point states that NCP - BCP + RCP - CCP = 1. This method had previously[13] been applied to **1**, with the surprising result that no BCP can be identified in **1** along the path connecting C1 to C7. In recognition of this feature, **1** has become known as a no-bond homoaromatic species.[13] It remains contentious whether the topological interpretation of the electron density provided by this analysis necessarily relates to the best *chemical* description of the bonding. In any event, **3** also exhibits no bond critical point in the C1−C9 region (Figure 1), although the predicted separation of these nuclei is in fact much shorter than that for **1** (Web-enhanced Table 1). The AIM analysis does however provide precisely one RCP for **3** (X=CH_2), and its coordinates provide a convenient location for measuring the magnetic properties of this system via the NICS (nucleus independent chemical shift).[8] Thus the NICS(rcp) of **3** has the value of −11.3 ppm (in comparison, benzene has a value at the equivalent ring centroid of ∼−10, **1** sustains a value of −11.5 and **2** of −10.9 ppm). By these various measures, **3** (X=CH_2) is clearly aromatic and more specifically homoaromatic.

It has recently been argued that a better chemical interpretation is provided not by the topology of the full electron density but by a related measure known as the electron localization function (ELF(r)).[15] This function provides information relating to localized electron pairs and therefore gives a direct insight into chemical bonding. In the density functional approach we are using here, ELF is calculated using the Pauli kinetic energy density. A consequence of the Pauli principle is that the probability of finding two electrons of opposite spin in the same region of space is increased, which leads to greater Coulomb repulsion between these two electrons and results in a larger kinetic energy (than if the Pauli principle had been ignored). It is this excess electronic kinetic energy value, relative to a homogeneous electron gas (of the same density), that defines the DFT-based ELF, which has been formulated to take values between 0 and 1. The greater the excess kinetic energy (and therefore the greater the Pauli repulsion and concomitant likelihood of finding pairs of electrons of opposite spin), the closer the ELF function is to 1. As with AIM, critical points can be identified in the properties of this function, but in fact a more useful analysis is the localization domain reduction tree (LDRT), which is used to identify so-called bifurcation thresholds for basins in the ELF topology.[15a,b] As ELF(r) is increased from 0 toward 1.0, the thresholds at which the ELF basin in the region of any putative bond first appears (bifurcates) and then vanishes are useful indications of the nature of the chemical bonding there. Thus the all-electron valence basins for most conventional bonds vanish to a point at ELF(r) values of ∼0.94−0.95, whereas weaker interactions such as hydrogen bonds, agostic interactions, or π-stacking may not even sustain the formation of discrete basins. The basins themselves can be one-centered (monosynaptic; lone pairs), two-centered (disynaptic), or three-centered (trisynaptic). Appropriate integration over the volume of any basin yields the total number of electrons associated with each basin.

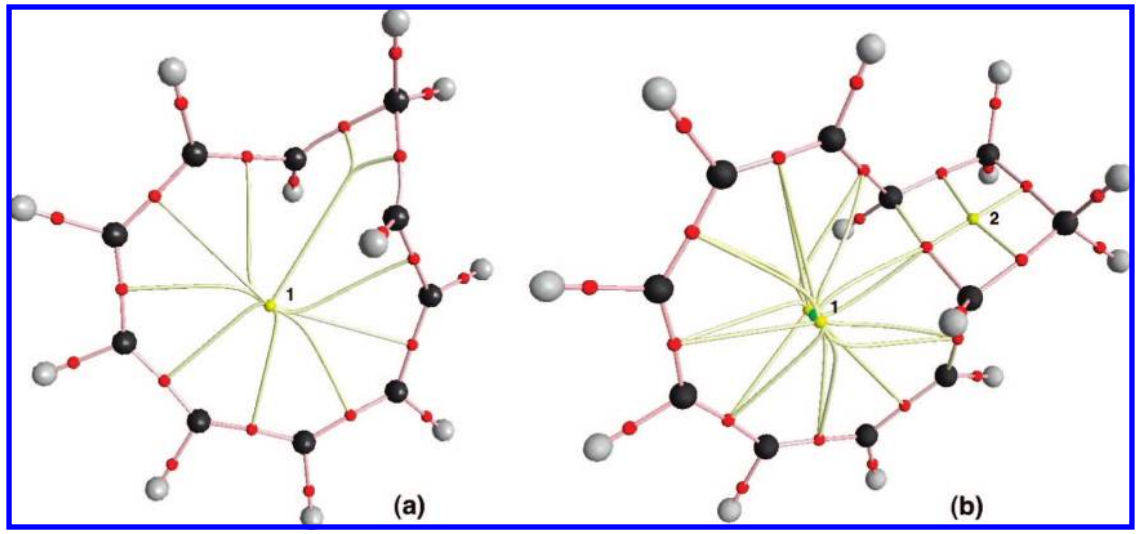

Figure 1. Critical points for (a) **3**, X=CH_2 and (b) **3**, X=CH_2 CH_2. Bond critical points are shown in red, ring critical points in yellow, and cage critical points in green. The ρ(r) values (in e.Å^{-3}, B3LYP/6−31G(d,p)), at RCP points (yellow) 1 are 0.004, and 0.072 at point 2. In (b), the helicity of the system causes the RCP to split into two such points, connected by a CCP (green). Such behavior has been previously noted.[14]

When this procedure is applied to **3**, X=CH_2, a disynaptic all-electron basin is identified in the region of the C1−C9 bond and is designated V(C1,C9). It has a ELF(r) 0.675 for its bifurcation point, 0.776 at its vanishing point, and a value of 0.79 electrons for the basin integration (Web-enhanced Table 1). This relatively low excess value for the Pauli repulsion energy does correspond to the chemical interpretation that the C1−C9 "bond" is significantly more delocalized than a conventional single bond type. The 0.79e basin population corresponds nicely to the concept of a π-bond shorn of its underlying 2-electron σ-framework (i.e., a homoaromatic bond); the V(CC) basin integrations for the other C−C bonds in the ring indeed do range from 2.4 to 2.9e, corresponding to more conventional two-center-three-electron aromatic bonds.

It is also possible to perform the ELF analysis by specifying a subset of the occupied molecular orbitals, such as the π-manifold.[16] Four occupied MOs for **3**, X=CH_2 can be identified as $\sim\pi$ (Figure 2) although mixing from the C−H σ-manifolds is also clearly apparent (*e.g.* Figure 2d). Simple Huckel MO theory predicts that π-orbitals in a Möbius cycle will occur as degenerate pairs,[3] although in practice this degeneracy is always broken.[17] The most stable π-MO pair (orbitals 31, 32, Figure 2) each has one node which occurs at one of the bisection points of the cycle by the C_2 axis of symmetry, and the less stable of this pair (albeit by only 0.1 eV, Figure 2c) has this node in the C1−C9 homobond region, again coincident with the C_2 axis. This type of behavior is also manifested by the parent ion **2**.[17]

ELF(r)$_\pi$ obtained using just this orbital subset exhibits bifurcation values for most of the π-like synaptic basins over the range 0.80−0.88, compared to the characteristically aromatic value for V(C,C)$_\pi$ of 0.91 reported for benzene.[16] There are differences however in behavior compared to a planar aromatic such as benzene. For example, whereas the benzene ELF(r)$_\pi$ bifurcation into two equal but separate disynaptic π-valence basins (one above, the other below the plane of the ring) must occur at the same threshold, the process for a helical Möbius system involves no such plane of symmetry and the two opposing lobes of the π-system may separate at different thresholds. This difference is illustrated by the ELF(r)$_\pi$ isosurface at 0.47 for **3**, X=CH_2 (Web-enhanced Table 1), which represents the bifurcation of the "inside" or endocyclic lobe of the C1−C9 π-basin away from its neighbors, but leaving a 5-center basin representing much of the rest of the original cyclic π-density still unseparated (Figure 4). The previously reported ELF(r)$_\pi$-based aromaticity scale[16] interprets a value of 0.47 as verging on the antiaromatic, but the low bifurcation value for this particular ELF basin may instead be characteristic of either homoaromaticity or of Möbius topology or both. Thus the corresponding values for **2** (0.33 for the initial π-bifurcation and 0.95 for its completion) are very similar to those for **3**, X=CH_2. What is clear is that while a simple Möbius aromaticity scale based on ELF(r)$_\pi$ values is unlikely to be accurately quantitative, the ELF-inferred homoaromaticity of **3**, X=CH_2 certainly approximates to that of benzene in most regards.

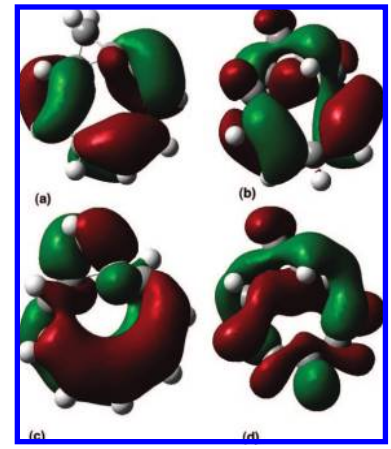

Figure 2. π-like molecular orbitals for **3**, X=CH_2 for (a), orbital 35, (b), orbital 34, (c) orbital 32, and (d) orbital 31, contoured at a threshold of 0.02 au at the B3LYP/6−31G(d,p) level.

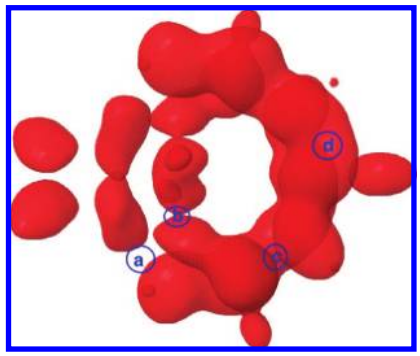

Figure 3. ELF$_\pi$=0.495 isosurface for **3**, X=CH$_2$, revealing that bifurcation of the π-surface at point (a) has already passed, whereas those at points (b) and (c) are on the cusp, and that at e.g. point (d) and others are still some way off. The isosurface prior to bifurfurcation has the topology of a one component torus knot.[17]

The preceding ELF and AIM analyses have revealed a clear divergence for **3**. Whereas no AIM C1−C9 bond critical point exists, ELF shows a clear disynaptic valence basin in this region, occupied by ∼1 π-electron. This contrasts with the AIM and ELF analyses (Web-enhanced Table 1) of the homotropylium cation **1**, the former sustaining no C1−C7 bond critical point, and the latter concurring with absence of a C1−C7 disynaptic basin. Therefore while **1** is indeed well described as a no-bond homoaromatic system, **3** arguably should not be so described.

Another measure of a Möbius electronic system is the properties of its π-AO ribbon as defined by the cyclic array of the p-atomic orbital basis and a topological property of that ribbon known as the linking number L$_k$. An important theorem introduced by White, Fuller, and Cãlugãreanu[18] defines a decomposition of L$_k$ into noninteger total twist (T$_w$) and writhe (W$_r$) components, according to

$$L_k = T_w + W_r$$

The two (noninteger) components of L$_k$ are obtained by integration of the appropriate functions of the ribbon coordinates, with T$_w$ being the integral of all local torsions γ around the center line of the basis set ribbon and W$_r$ (known as the writhe of the system) being a nonlocal property obtained by a double-integration.[19] The writhe of the ring describes the extent to which the center line of the basis set ribbon projects from 2D into 3D space. Expressed in units of π, a value of L$_k$ =1 corresponds to the conventional description of a single half-twist Möbius system, while larger values are often referred to as the corresponding higher-order Möbius systems. Using the previously described protocol,[19] the values for **3**, X=CH$_2$ are computed as L$_k$ = 1π, T$_w$=1.13, and W$_r$ = −0.13, this being the first homoaromatic system analyzed in this manner. The degree by which W$_r$ modifies the value of T$_w$ (they are normally but not necessarily of the same sign) can be most simply interpreted in terms of how much the (unfavorable) reduction in p$_\pi$-p$_\pi$ AO overlaps brought about by T$_w$ torsion can instead be converted into (presumably the more favorable) bending deformations which are a feature of writhe.[19] In this example, little such conversion has taken place; the system being almost a pure half-twist Möbius molecule, with little projection of the torsions into the writhe of 3D space. This might be contrasted with the values for **2** itself, which were reported[19] as L$_k$ = 1π, T$_w$=0.73, and W$_r$ = 0.27π, indicating some relief of (overlap reducing) p$_\pi$-p$_\pi$ torsions.

2.2. Other Möbius Homoaromatics Based on 3. With these methodologies established for characterizing the species, we next explored the results of varying the nature of the bridging group X. For the larger bridge X=CH$_2$−CH$_2$, similar AIM results were obtained in all but one regard. The C1−C9 bond length was slightly longer, Δ_r was somewhat larger, but the NICS(rcp) was still characteristic of an aromatic system. However, the system now **did** exhibit (Figure 1b) a BCP in the C1−C9 region, despite the nuclei being further apart! The ELF(r) V(C1,C9) basin disappearance threshold of 0.879 and a basin integration of 1.17e also indicated somewhat more localized bonding, tending toward **4**.

Our task now became one of exploring whether chemical characteristics for predicting whether a BCP might be expected in any given bonding region can be defined. This was achieved by systematically varying the electron demand of X, *via* both the central atoms, and their substituents. Thus **3**, X=C(SiH$_3$)$_2$ increases the electron donation of the substituent, and the critical point analysis now changes quantitatively, in revealing two additional critical points compared to X=CH$_2$, comprising one BCP and one RCP. It

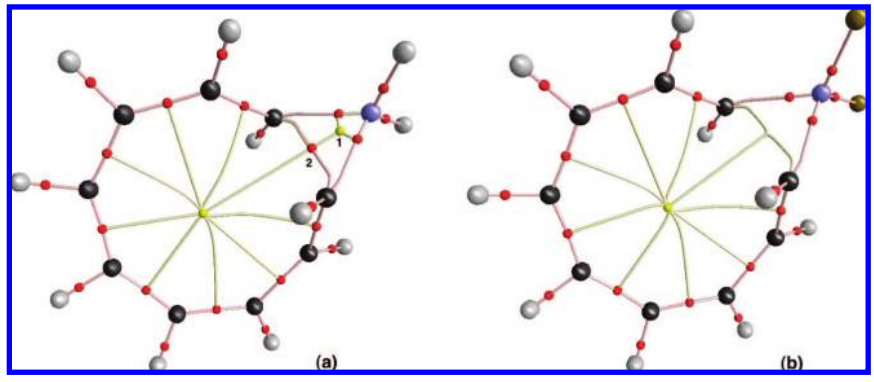

Figure 4. Critical points for (a) **3**, X=BH$_2$ and (b) **3**, X=BF$_2$. The ρ(r) values (in e.Å^{-3}, B3LYP/6−31G(d,p)), at RCP point (yellow) 1 and BCP point 2 (red) are 0.134 and 0.140, respectively. In (b), these two points have self-annihilated as a result of replacing H by F.

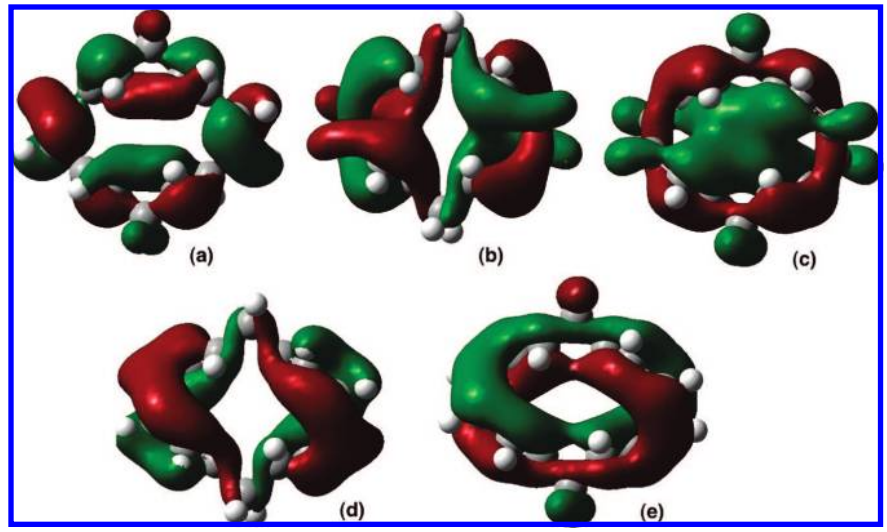

Figure 5. π-like molecular orbitals for **5**, X=CH_2 for (a), orbital 49, (b), 48, (c) 47, (d) 46, and (e) 45, contoured at a threshold of 0.02 au at the B3LYP/6−31G(d,p) level. Orbital 45 has the topology of a two-component torus link.

can be seen from the Poincaré-Hopf condition that creating one of each does not change the overall adherence to this rule. One can draw a (loose) analogy to the creation and subsequent annihilation of virtual pairs of nuclear particles. In our case, if the pair of BCP + RCP points is relatively close in space and in value of ρ(r), they will be prone to self-annihilate.[14] Looked at in this manner, the presence (or absence) of a BCP+RCP pair is merely the consequence of subtle changes in the electron density in the region of the pair and not a fundamental of the bonding of the molecule. Thus increasing the electron density in the C1−C9 region enables the creation of such a BCP+RCP pair, and it also increases the ELF V(C1,C9) threshold and the basin integration (0.98). Conversely, removing electron density might be expected to encourage any geometrically close BCP+RCP pair to self-annihilate.

The remaining entries in the Web-enhanced Table 1 provide support for this hypothesis. Thus the electron releasing **3**, X=BH_2 induces the creation of a BCP+RCP pair in the C1−C9 region, although the character of the ELF V(C1−B−C9) basin is tri- rather than disynaptic. The same effect is also obtained for the homotropylium analogue **1**, X=BH_2. The less electropositive **3**, X=BF_2 does not induce BCP+RCP creation (Figure 4 b,c), but it retains the trisynaptic nature of the valence basin. When the central atom in X is B or Al, the overall charge on the system is zero (it being zwitterionic), and the NICS(rcp) and Δ_r values suggest even more highly homoaromatic molecules. Indeed, even the anionic **3**, X=BeH_2 seems to sustain the effect.

The ELF(r)$_{C1-C9}$ basins also proved sensitive to substitution (Web-enhanced Table 1). If electron density is injected into this region, the vanishing threshold for the basin increases (toward that of a localized single bond). Conversely, electron withdrawal could inhibit even the formation of any basin in this region (e.g., X=SiF_2, AlF_2), and some basins have scarcely formed before they vanish at higher ELF(r) values (X=BH_2). These features suggest that analysis of ELF(r)$_{C1-C9}$ basins provides a more sensitive chemical probe than that provided purely by the presence or absence of bond critical points in the AIM analysis.

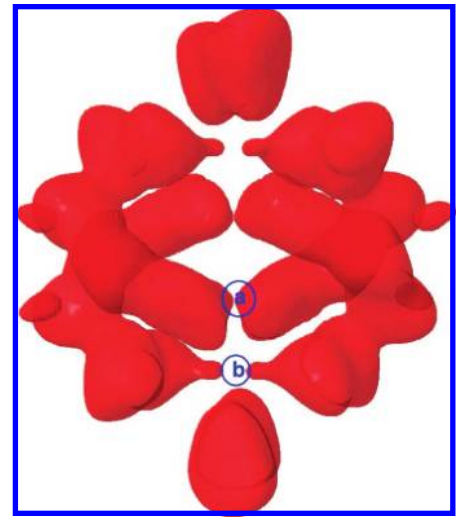

Figure 6. ELF(r)$_\pi$=0.275 isosurface for **5**, X=CH_2, revealing that bifurcation of the endocyclic π-torus at point (a) is at the cusp, while that of the exocyclic π-torus (b) has already passed. The isosurface prior to bifurcation has the topology of a two-component torus link.

2.3. Möbius Bishomoaromatics Based on 5. The concept can also be extended to Möbius bis-homoaromaticity. The dication **5**, X=CH_2 comprises two 5π monocationic components in which cyclic conjugation and hence aromaticity occurs across two CH_2 bridges. Having D_2-symmetry, it represents a double half-twist Möbius homoaromatic, for which a 4n+2 electron selection rule applies.[19] It sustains a large NICS(rcp) value of −15.8 ppm indicating a strong diatropic ring current, similar to that previously reported for a related nonhomoaromatic Möbius double half-twist system.[18,20] The neutral **5**, X=BH_2 is even more homoaromatic, with a shorter C−C homo bond length and a larger NICS(rcp) value. As before with **3**, the dicationic carbocyclic system (X=CH_2) shows no AIM bond-critical point, whereas the neutral boron system (X=BH_2) does. No ELF(r) all-electron disynaptic basin in the homobond region was located for X=CH_2, and so a dissection into its π-component was undertaken. The first five occupied MOs are in fact all π in

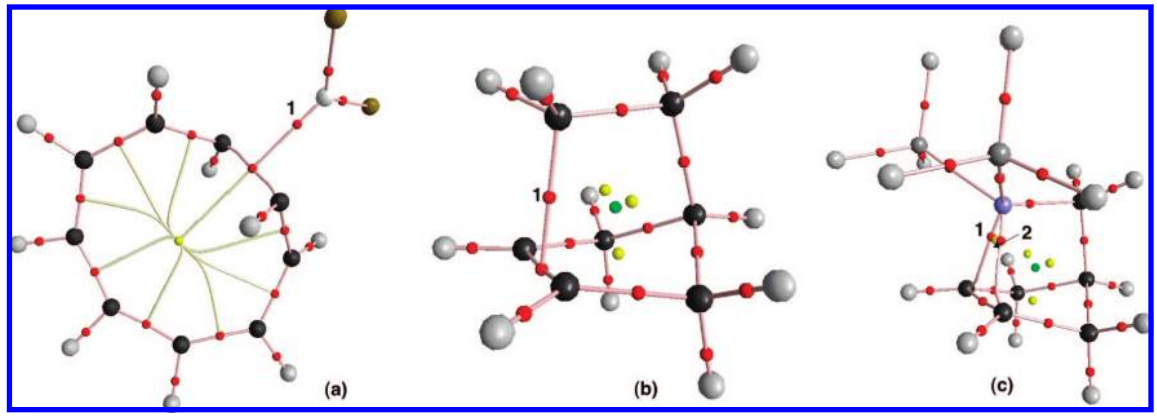

Figure 7. Critical points for (a) **3**, X=BeF_2, (b) **6**, Z=C,Y=H. (c) **6**, Z=B,Y=SiH_3. The ρ(r) values (in e.$Å^{-3}$, B3LYP/6−31G(d,p)), at BCP point 1 (red) are 0.050, 0.085, and 0.105, respectively, and for RCP 2 (C), 0.105. Self-annihilation of points 1 and 2 in (c) results in point 1 in (b) remaining.

character (Figure 5). Noteworthy is the most stable of these (Figure 5e), which is cyclically continuous, and forms what is called a two component torus link that is identical in appearance to that described previously for the nonhomo forms.[19]

An ELF(r)$_\pi$ bufurcation takes place at an isosurface value of 0.275 (Figure 6) being that of the original π-torus at the two endocyclic regions of the homobond (the exocyclic torus having already bifurcated). The remaining π-torus does not fully bifurcate into basins until 0.986, a value even higher than that for benzene.[16] It is indeed tempting to conclude, by this measure at least, that a bis-homoaromatic system such as **5** is substantially more aromatic than even benzene!

As with **3**, a linking analysis for **5**, X=CH_2 reveals $L_k = 2\pi$, T_w=1.75, and $W_r = 0.25$, which again indicates relatively little of the double-half-twist of the ring has been transformed to writhe.

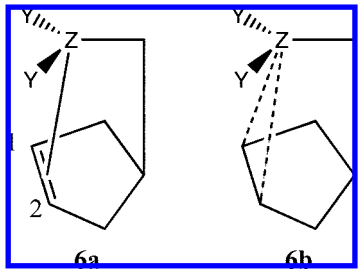

2.4. Comparisons with the Norbornyl Cation 6. The specific example of **3**, X=BeF_2 gave the same number of BCPs as did X=CH_2, but they occurred in *different regions*. Whereas no BCP was present along the C1−C9 region for X=CH_2, two BCPs were located along C1-X and C9-X (Figure 1a). For X=BeF_2, one BCP is located in the C1−C9 region, and the second BCP lies along the path apparently connecting the first BCP to X (Figure 7a, point 1). This rather odd AIM-BCP behavior has in fact been computed[21] in another cationic system, the norbornyl cation **6** (also famously associated with Winstein). Two representations of the symmetrical species (in which the group ZY_2; Z=C^+, Y=H bridges symmetrically across the C1−C2 bond) have been argued over. Representation **6a** is that of a π-complex, in which the pair of π-electrons in the C1−C2 alkene donate into the vacant p-orbital on Z. The other, **6b**, is a nonclassical two-electron-three-center interpretation, in which (weaker) bonding is considered as occurring between each of C1 and C2 and Z. In terms of the AIM critical point analysis, **6a** results in a BCP along the C1−C2 path, and a second BCP occurs along the path connecting the first BCP and Z (Figure 7b). This is the result recovered for Z=C^+, Y=H. From our experiences above, one might expect a different result to be obtained if ZY_2 were to be made more electron releasing. Thus for the (neutral) system Z=B, Y=SiH_3, just such is computed. An additional BCP + RCP pair is created, and BCPs now occur along C1−C2, C1-Z, and C2-Z, and a RCP occurs at the centroid of this 3-membered ring, this effectively being representation **6b** (Figure 3c). Thus these two representations are therefore really just small, but subtle variations in the electron density topology, which differ only in whether a BCP+RCP pair is created or annihilated. Because this creation/annihilation only occurs when the critical points are close (it is estimated <0.2 Å),[14] this effect is only likely to be encountered for small, e.g. 3-membered rings; it no longer occurs for the larger 4-ring (**3**, X=CH_2CH_2).

3. Conclusions

The hitherto unexplored genre of Möbius homoaromaticity emerges as a new addition to the many diverse types of molecule that are regarded as having aromatic character. The effect appears equally prominent in cationic, neutral, and anionic molecules and also appears to sustain higher-order half-twists in the Möbius topologies, corresponding to e.g. bis-homoaromaticity. Unlike Hückel homoaromatics, the Möbius forms are intrinsically chiral (dissymmetric). Given the recent syntheses of a variety of Möbius single and higher order twist systems,[6] a speculation of whether any homo-Möbius aromatic might be synthetically accessible appears reasonable.

4. Computational Details

Calculations were performed at the B3LYP[22] DFT level and 6−31G(d,p) or aug-cc-pVTZ basis set level,[23] as implemented in the Gaussian 03 (revision E.01) program.[24] AIM critical points and the molecular graphs that map their connectivity were obtained by exporting a WFN file from Gaussian and importing into AIM2000.[25] The ring critical point coordinates so obtained were used to evaluate the NICS(rcp) values using Gaussian 03.[8]

ELF(r) and ELF(r)$_\pi$ cubes were calculated using Dgrid[26] via a FCHK file exported from Gaussian and visualized at differing isosurface values with VMD[27] or Jmol.[28] Basin integration was performed using TopMod.[29] The data files and coordinates are all available *via* the digital repository entries[30] to be found in the Web-enhanced Table 1.

References

(1) Winstein, S. *J. Am. Chem. Soc.* **1959**, *81*, 6524–6525. DOI: 10.1021/ja01533a052.

(2) (a) Childs, R. F. *Acc. Chem. Res.* **1984**, *17*, 347–352. DOI: 10.1021/ar00106a001. (b) Cremer, D.; Kraka, E.; Slee, T. S.; Bader, R. F. W.; Lau, C. D. H.; Nguyen-Dang, T. T.; MacDougall, P. J. *J. Am. Chem. Soc.* **1983**, *105*, 5069–5075. DOI: ja00353a036. (c) Lepetit, C.; Silvi, B.; Chauvin, R. *J. Phys. Chem. A* **2003**, *107*, 464–473. DOI: 10.1021/jp0265211. (d) Cremer, D.; Reichel, F.; Krafka, E. *J. Am. Chem. Soc.* **1991**, *113*, 9459–9466. DOI: 10.1021/ja00025a006. (e) Geier, J. *J. Phys. Chem. A* **2006**, *110*, 9273–9281. DOI: 10.1021/jp061498f.

(3) Heilbronner, E. *Tetrahedron Lett.* **1964**, 1923–1928. DOI: 10.1016/S0040-4039(01)89474-0.

(4) (a) Zimmerman, H. E. *J. Am. Chem. Soc.* **1966**, *88*, 1564–1565. DOI: 10.1021/ja00959a052. (b) Zimmerman, H. E. *J. Am. Chem. Soc*. **1966**, *88*, 1566−1567. DOI: 10.1021/ja00959a053. (c) Zimmerman, H. E. *Tetrahedron* **1982**, *38*, 753–8. DOI: 10.1016/0040-4020(82)80155-5.

(5) (a) Rzepa, H. S. *Chem. Rev.* **2005**, *105*, 3697–3715. DOI: 10.1021/cr030092l. (b) Herges, R. *Chem. Rev.* **2006**, *106*, 4820–4842. DOI: 10.1021/cr0505425. (c) Ajami, D.; Oeckler, O.; Simon, A.; Herges, R. *Nature* **2003**, *426*, 819. (d) Ajami, D.; Hess, K.; Köhler, F.; Näther, C.; Oeckler, O.; Simon, A.; Yamamoto, C.; Okamoto, Y.; Herges, R. *Chem. Eur. J.* **2006**, *12*, 5434.

(6) (a) Kastrup, C. J.; Oldfield, S. V.; Rzepa, H. S. *Dalton Trans.* **2002**, 2421–2422. (b) Hall, D.; Rzepa, H. S. *Org. Biomol. Chem.* **2003**, *1*, 182–185. (c) Kui, S. C. F.; Huang, J.-S.; Sun, R. W.; Zhu, N.; Che, C. M. *Angew. Chem., Int. Ed.* **2006**, *45*, 4663–4666. (d) Park, J. K.; Yoon, Z. S.; Yoon, M. -C.; Kim, K. S.; Mori, S.; Shin, J.-Y.; Osuka, A.; Kim, D. *J. Am. Chem. Soc.* **2008**, *130*, 1824–1825. (e) Tunyogi, T.; Deák, A.; Tárkányi, G.; Király, P.; Pálinkás, G. *Inorg. Chem.* **2008**, *47*, 2049–2055. DOI:10.1021/ic702059v. (f) John, R. P.; Park, M.; Moon, D.; Lee, K.; Hong, S.; Zou, Y.; Hong, C. S.; Lah, M. S. *J. Am. Chem. Soc.* **2007**, *129*, 14142–14143. (g) Rzepa, H. S. *Org. Lett.* **2008**, *10*, 949–952. (h) Rzepa, H. S.; *Inorg. Chem*. **2008**,in press. (i) Stepien, M.; Latos-Grazynski, L.; Sprutta, N.; Chwalisz, P.; Szterenberg, L. *Angew. Chem., Int. Ed.* **2007**, *46*, 7869–7873. (j) Pacholska-Dudziak, E.; Skonieczny, J.; Pawlicki, Szterenberg, M. L.; Ciunik, Z.; Latos-Grazynski, L. *J. Am. Chem. Soc.* **2008**, *130*, 6182–6195.

(7) Mauksch, M.; Gogonea, V.; Jiao, H.; von, P.; Schleyer, R. *Angew. Chem. Int. Ed.* **1998**, *239*, 5–2397. DOI:10.1002/(SICI)1521-3773(19980918)37:17<2395::AID-ANIE2395>3.0.CO;2-W.

(8) (a) Schleyer, P. v. R.; Maerker, C.; Dransfeld, A.; Jiao, H.; van Eikema, H.; Nicolaas, J. R. *J. Am. Chem. Soc.* **1996**, *118*, 6317–6318. DOI: 10.1021/ja960582d. (b) Chen, Z.; Wannere, C. S.; Corminboeuf, C.; Puchta, R.; Schleyer, P. v. R. *Chem. Rev.* **2005**, *105*, 3842–3888. DOI: 10.1021/cr030088+For a comparison of NICS with a range of other aromaticity indices, see: (c) Bultinck, P. *Faraday Discuss.* **2007**, *135*, 347–365. DOI: 10.1039/b609640a.

(9) Allan, C. S. M.; Rzepa, H. S. J. Org. Chem. **2008**, *73*, 6615–6622. DOI: 10.1021/j0801022b.

(10) (a) Winstein, S.; Kaesz, H. D.; Kreiter, C. G.; Friedrich, E. C. *J. Am. Chem. Soc.* **1965**, *87*, 3267–9. DOI: 10.1021/ja01092a060. (b) Aumann, R.; Winstein, S. *Tetrahedron Lett.* **1970**, *11*, 903–6. DOI: 10.1016/S0040-4039(01)97862-1.

(11) (a) Poater, J.; Duran, M.; Sola, M.; Silvi, B. *Chem. Rev.* **2005**, *105*, 3911–3947. DOI: 10.1021/cr030085x. (b) Bader, R. F. W. *Atoms in Molecules: a Quantum Theory*; Oxford University Press: Oxford, U.K., 1990. (c) Popelier, P. L. A. *Atoms in Molecules: an Introduction*; Prentice- Hall: London, 2000.

(12) (a) Becke, A. D.; Edgecombe, K. E. *J. Chem. Phys.* **1990**, *92*, 5397–5403. DOI: 10.1063/1.458517. (b) Savin, A.; Jepsen, O.; Flad, J.; Andersen, O. K.; Preuss, H.; von Schnering, H. G. *Angew. Chem., Int. Ed.* **1992**, *31*, 187–188.

(13) (a) Lepetit, C.; Silvi, B.; Chauvin, R. *J. Phys. Chem. A* **2003**, *107*, 464–473. DOI: 10.1021/jp026521l. For a more general review of the electronic properties of homoaromaticity, see: (b) Cremer,D.; Childs, R. F.; Kraka, E. Chemistry of the Cyclopropyl Group;Rappaport, Z., Ed.; 1995; Vol. 2, pp 339−410.

(14) Castillo, N.; Matta, C. F.; Boyd, R. J. *Chem. Phys. Lett.* **2005**, *409*, 265–269. DOI: 10.1016/j.cplett.2005.04.088.

(15) (a) Savin, A.; Silvi, B.; Colonna, F. *Can. J. Chem.* **1996**, *74*, 1088–1096. DOI: 10.1139/v96-122. (b) Fuster, F.; Silvi, B. *Theor. Chem. Acc.* **2000**, *104*, 13–21. DOI: 10.1007/s002149900100. (c) Calatayud, M.; Andres, J.; Beltran, A.; Silvi, B. *Theor. Chem. Acc.* **2001**, *105*, 299–308. DOI: 10.1007/s002140000241. (d) Kohout, M.; Wagner, F. R.; Grin, Y. *Theor. Chem. Acc.* **2002**, *108*, 150–156. DOI: 10.1007/s00214-002-0370-x. (e) Cioslowski, J.; Matito, E.; Sola, M. *J. Phys. Chem. A* **2007**, *111*, 6521–6525. DOI: 10.1021/jp0716132.

(16) Santos, J. C.; Tiznado, W.; Contreras, R.; Fuentealba, P. *J. Chem. Phys.* **2004**, *120*, 1670–1673. DOI: 10.1063/1.1635799.

(17) Wannere, C. S.; Rzepa, H. S.; Rinderspacher, B. C.; Paul, A.; Schaefer, H. F.; Schleyer, P. v. R.; Allan, C. S. M., submitted for publication.

(18) (a) White, J. H. *Am. J. Math.* **1969**, *91*, 693–728. (b) Cālugāreanu, G. *Czech. Math. J.* **1961**, *11*, 588–625. (c) Fuller, F. *Proc. Natl. Acad. Sci. U.S.A.* **1971**, *68*, 815–819. (d) Pohl, W. *Indiana Univ. Math. J.* **1968**, *17*, 975–985.

(19) Rappaport, S.; Rzepa, H. S. *J. Am. Chem. Soc.* **2008**, *130*, 7613–7619. DOI: 10.1021/ja10438j.

(20) Rzepa, H. S. *Org. Lett.* **2005**, *7*, 4637–39. DOI: 10.1021/ol0518333.

(21) (a) Werstiuk, N. H.; Muchall, H. M. *THEOCHEM* **1999**, *463*, 225–229. DOI: 10.1016/S0166-1280(98)00625-3. (b) Werstiuk, N. H.; Muchall, H. M.; Noury, S. *J. Phys. Chem., A* **2000**, *104*, 11601–11605. DOI: 10.1021/jp001978l. (c) Firme, C. L.; Antunes, O. A. C.; Esteves, P. M. *J. Phys. Chem. A* **2008**, *112*, 3165–3171. DOI: 10.1021/jp710606n.

(22) Becke, A. D. *J. Chem. Phys.* **1993**, *98*, 1372–5648. DOI: 10.1063/1.464304.

(23) Dunning, T. H. *J. Chem. Phys.* **1989**, *90*, 1007–1023. DOI: 10.1063/1.456153.

(24) Frisch, M. J.; Trucks, G. W.; Schlegel, H. B.; Scuseria, G. E.; Robb, M. A.; Cheeseman, J. R.; Montgomery, J. A., Jr.; Vreven, T.; Kudin, K. N.; Burant, J. C.; Millam, J. M.; Iyengar, S. S.; Tomasi, J.; Barone, V.; Mennucci, B.; Cossi, M.; Scalmani, G.; Rega, N.; Petersson, G. A.; Nakatsuji, H.; Hada, M.; Ehara, M.; Toyota, K.; Fukuda, R.; Hasegawa, J.; Ishida, M.; Nakajima, T.; Honda, Y.; Kitao, O.; Nakai, H.;

Klene, M.; Li, X.; Knox, J. E.; Hratchian, H. P.; Cross, J. B.; Bakken, V.; Adamo, C.; Jaramillo, J.; Gomperts, R.; Stratmann, R. E.; Yazyev, O.; Austin, A. J.; Cammi, R.; Pomelli, C.; Ochterski, J. W.; Ayala, P. Y.; Morokuma, K.; Voth, G. A.; Salvador, P.; Dannenberg, J. J.; Zakrzewski, V. G.; Dapprich, S.; Daniels, A. D.; Strain, M. C.; Farkas, O.; Malick, D. K.; Rabuck, A. D.; Raghavachari, K.; Foresman, J. B.; Ortiz, J. V.; Cui, Q.; Baboul, A. G.; Clifford, S.; Cioslowski, J.; Stefanov, B. B.; Liu, G.; Liashenko, A.; Piskorz, P.; Komaromi, I.; Martin, R. L.; Fox, D. J.; Keith, T.; Al-Laham, M. A.; Peng, C. Y.; Nanayakkara, A.; Challacombe, M.; Gill, P. M. W.; Johnson, B.; Chen, W.; Wong, M. W.; Gonzalez, C.; Pople, J. A. *Gaussian 03, Revision E.01*; Gaussian, Inc.: Wallingford, CT, 2004.

(25) For computer programs, see: (a) Biegler-König, F. W.; Schönbohm, AIM2000. The program can be downloaded at http://www.aim2000.de/ (accessed 08/28/08). (b) Keith, T. A., AIMAll (Version 08.04.21), 2008. The program can be downloaded at http://aim.tkgristmill.com (accessed 08/28/08).

(26) For Computer Program, see: (a) Kohout, M. DGrid, version 4.3; 2008.

(27) For Computer Program, see: (a) Humphrey, W.; Dalke, A.; Schulten, K. *J. Mol. Graphics* **1996**, *14*, 33–38, Version 1.8.6, 2007. The program can be downloaded at http://www.ks.uiuc.edu/Research/vmd/ (accessed 08/28/08).

(28) For Computer Program, see: Hanson, R., Ed.; 2008. The program can be downloaded at http://jmol.sf.net/ (accessed 08/28/08).

(29) For Computer Program, see: Noury, S.; Krokidis, X.; Fuster, F.; Silvi, B. TopMoD package; Universite Pierre et Marie Curie, 1997. The program can be downloaded athttp://www.lct.jussieu.fr/pagesperso/silvi/topmod.html (accessed 08/28/08).

(30) Rzepa, H. S.; Downing, J.; Tonge, A.; Cotterill, F.; Harvey, M. J.; Murray-Rust, Morgan, P.; Day, N. J. Chem. Inf. Model. **2008**, *48*, 1571–1581. DOI: 10.1021/ci7004737.

CT8001915